

# Structure Development during Crystallization and Solid-State Processing of Poly(glycolic acid)

H. Montes de Oca,<sup>1\*</sup> I. M. Ward,<sup>1</sup> R. A. Chivers,<sup>2</sup> D. F. Farrar<sup>2</sup>

<sup>1</sup>IRC in Polymer Science and Technology, School of Physics and Astronomy, University of Leeds, Leeds LS2 9JT, United Kingdom

<sup>2</sup>Smith and Nephew Research Centre, York Science Park, Heslington, York YO10 5DF, United Kingdom

Received 11 November 2007; accepted 21 July 2008

DOI 10.1002/app.29000

Published online 17 October 2008 in Wiley InterScience (www.interscience.wiley.com).

**ABSTRACT:** DSC and time-resolved WAXS and SAXS are used to study the structure development during isothermal crystallization of poly(glycolic acid) (PGA) in the temperature range 180–195°C. It is shown that the crystallization rate increases with degree of supercooling in the temperature range of consideration. WAXS and DSC crystallinity measurements agree well and a final crystallinity of 50% is found independently of the crystallization temperature. In-situ SAXS measurements indicate that for PGA the final crystal thickness approaches a limiting value of 70 Å independent of the crystallization temperature in the range 195–180°C. The material develops a well-defined

lamellar structure during crystallization at the highest crystallization temperature under study (195°C). We show that by increasing the degree of supercooling it is possible to hinder the formation of the lamellar structure and crystals, resulting in a less ordered structure. We report that PGA fibers with elastic modulus in the range 20–25 GPa can be prepared by adequate control of the structure before solid-state plastic deformation. © 2008 Wiley Periodicals, Inc. *J Appl Polym Sci* 111: 1013–1018, 2009

**Key words:** polyesters; crystallization; biomaterials; structure–property relations

## INTRODUCTION

Poly(glycolic acid) (PGA) is a semicrystalline polyester with good mechanical and degradative properties. It is biocompatible and in the body degrades via a hydrolysis reaction in which glycolic acid (GA) is the primary degradation product.<sup>1</sup> GA is decomposed in the carbohydrate cycle within the body, making PGA and its copolymers very attractive for use in biomedical applications. Other applications of these materials include drug delivery carriers and scaffolds for cell culture.<sup>2,3</sup>

### Poly(glycolic acid)

Previous X-ray diffraction studies of PGA indicate that two planar zigzag molecules pass through an orthorhombic unit cell with dimensions  $a = 5.22$  Å,  $b = 6.19$  Å, and  $c = 7.02$  Å (fiber axis). The chain axis has a twofold screw symmetry along the  $c$ -axis

and the first chain lies on the  $ac$  plane at  $b/4$  whereas the second chain, which is the mirror image of the first chain rotated 180° about  $c/2$ , lies on the  $ac$  plane at  $3b/4$ .<sup>4</sup> Recently, structural studies of highly oriented PGA by  $H^1$  NMR spectroscopy<sup>5</sup> suggested that the ester group may not necessarily acquire a trans-planar conformation; however, the deviations from this, if any, are small and difficult to elucidate by X-ray diffraction, but appeared during more refined structural calculations of proton–proton dipole interactions within the crystal.

Microscopy studies of the morphology of PGA crystallized at different temperatures have found that this polyester crystallizes as spherulites, hedrites, and hedritic rosettes depending on the crystallization conditions.<sup>6</sup> In 1980, Chu<sup>7</sup> published a brief study of the crystallization kinetics of PGA in the form of a suture (Dexon) at high undercooling by differential scanning calorimetry. Other calorimetric studies of importance on PGA have been published by Cohn et al.<sup>8</sup> and by Gilding and Reed.<sup>9</sup> More recently, Wang et al.<sup>10</sup> published a study of the morphological development of PGA and some of its copolymers using time resolved X-ray diffraction techniques.

Despite PGA's long history of clinical use as sutures and other medical implants only limited information about the structure–processing–properties relationships has been disclosed. Montes de Oca and

\*Present address: York Science Park, Heslington, York YO10 5DF, United Kingdom.

Correspondence to: H. Montes de Oca (horacio.montesdeoca@smith-nephew.com).

Contract grant sponsors: Consejo Nacional de Ciencia y Tecnología (CONACyT), México and Smith and Nephew, England.

Ward<sup>11</sup> prepared highly oriented PGA fibers with modulus of 25 GPa and reported the theoretical elastic constants of the PGA crystal, finding very good agreement between the theoretical elastic modulus along the chain axis (296 GPa) and the value obtained from a combination of experimental measurements and a two phase structural model (286 GPa). However, the authors did not report in detail the effects of the fiber structure before solid-state processing. In this article, we use a combination of isothermal differential scanning calorimetry (DSC) measurements, time-resolved WAXS, and SAXS to gain understanding of the structure development during isothermal crystallization of PGA. We show that under adequate crystallization conditions, PGA can be prepared with various structures, which are critical for obtaining highly oriented PGA fibers.

## EXPERIMENTAL METHODS

### Crystallization by DSC and X-rays

Isotropic PGA was provided by Smith and Nephew Research Center (York, England). PGA sheets  $0.5 \pm 0.01$  mm thick were prepared by compression molding at 240°C, respectively. Flat specimens  $10.000 \pm 0.005$  mg were cut and placed in an aluminium pan for differential scanning calorimetry (DSC) and for in-situ crystallization measurements by wide and small angle X-ray scattering (WAXS and SAXS, respectively) using synchrotron radiation.

DSC measurements were carried out using a Perkin Elmer DSC7 calibrated with indium. Variations in the concavity and slope of the baseline curve were corrected until a satisfactory flat baseline was obtained. For the in-situ crystallization studies by WAXS and SAXS, a Linkham DSC calibrated (England) with indium was employed. This device has been adapted in such a way that the X-rays pass through the DSC pan while a predefined temperature program is followed. To obtain complementary information by DSC, WAXS, and SAXS, the samples tested in the Perkin Elmer and in the Linkham cell followed the same temperature programs. A typical temperature program is as follows. The sample was heated from room temperature at 50°C/min to approximately 20°C above the observed melting temperature ( $T_m$ ) and held at this temperature for 2 min to ensure that no trace of crystals remained. The sample was rapidly quenched using a mixture of liquid nitrogen and air at 100°C/min to 20°C above the target crystallization temperature ( $T_c$ ). The sample was further cooled from  $T_c + 20^\circ\text{C}$  to  $T_c$  at 50°C/min and maintained at  $T_c$  while measuring the heat flow under isothermal conditions for a period of time long enough to ensure that crystallization can be considered completed.

Time resolved WAXS and SAXS measurements were undertaken in separate experiments at the station 16.1 of the Synchrotron Radiation Source ( $\lambda = 1.41 \text{ \AA}$ ) at the CLRC Daresbury Laboratory using a CCD camera (WAXS) and a two-dimensional RAPID area detector (SAXS). The CCD device was calibrated with high-density polyethylene and silicon powder and the RAPID area detector with wet-rat tail collagen. To cover the angular range of interest, a sample to detector distance of 3.5 m was chosen for the SAXS measurements and slit collimated X-rays were employed. Ion chambers were placed before and after the sample (SAXS only) to normalize the recorded intensities. For the WAXS measurements, the data collection time was chosen to be 10 s/frame. Sufficient data were collected to cover the whole crystallization event practically from the beginning until it can be considered to have finished. For SAXS measurements, a similar method was used but in this case the data collection times were chosen to be 30 s/frame.

### Structure and mechanical properties of PGA fibers

Amorphous PGA fibers were prepared by a extrusion process at 240°C, quenching the fibers in a water bath at room temperature and slowly collecting them in order to minimize molecular orientation and thermal and stress-induced crystallizations. Semicrystalline isotropic fibers were prepared by annealing amorphous fibers at constant length at 110°C for 30 min using a conventional fan assisted oven coupled to an Instron tensile testing apparatus. Oriented fibers were prepared using the zone drawing technique at 110°C described in our previous publication.<sup>11</sup> Briefly, in this technique a fiber is locally heated above the glass transition temperature and simultaneously drawn, resulting in a localized neck region where plastic deformation and molecular orientation occurs. The structure of oriented fibers was studied by WAXS. During WAXS measurements the fiber axis was inclined approximately 80° relative to the X-ray beam in order to observe pure meridional reflections. The elastic modulus was obtained using a conventional Instron tensile test apparatus operated at room temperature, at 10 mm/min with a gauge length of 200 mm.

## EXPERIMENTAL RESULTS AND DISCUSSIONS

### Isothermal crystallization

Figures 1 and 2 show the heat flow measurements and the time evolution of the DSC crystallinity [see eq. (1) below] during isothermal crystallization at various crystallization temperatures, respectively.

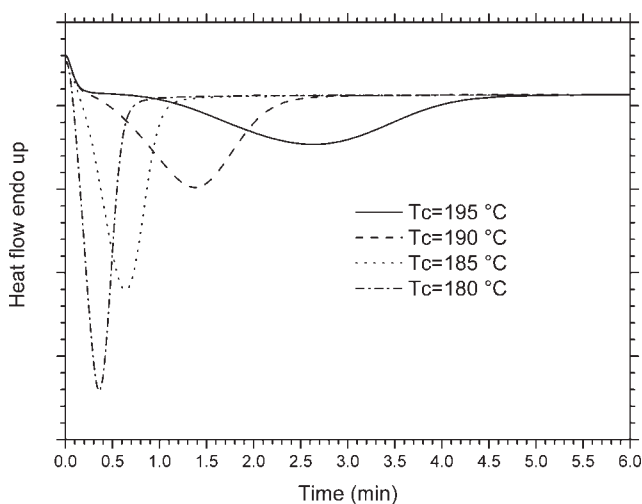


**Figure 1** Heat flow measurements during isothermal crystallisation of PGA at various temperatures.

$$X(t)\% = \frac{\int_0^t x(t^*) dt^*}{m\Delta H_m^0} \times 100 \quad (1)$$

where  $t$  is the time,  $x(t)$  is the measured value of the heat flow,  $m$  is the mass of the specimen and  $\Delta H_m^0$  is the heat of fusion of a perfect crystal (139 J/g for PGA<sup>8</sup>).

As can be seen in Figure 1, crystallization is faster at lower temperatures. Figure 2 on the other hand indicates that PGA achieves a final crystallinity of about 50% and that this is independent of the crystallization temperature ( $T_c$ ) in the temperature range under consideration (180–195°C).

Figure 3 (a,b) show the time resolved WAXS intensity profiles for PGA crystallized at 195°C and 180°C, respectively. As can be seen, at 180°C two clear peaks have developed after 24 s, whereas at

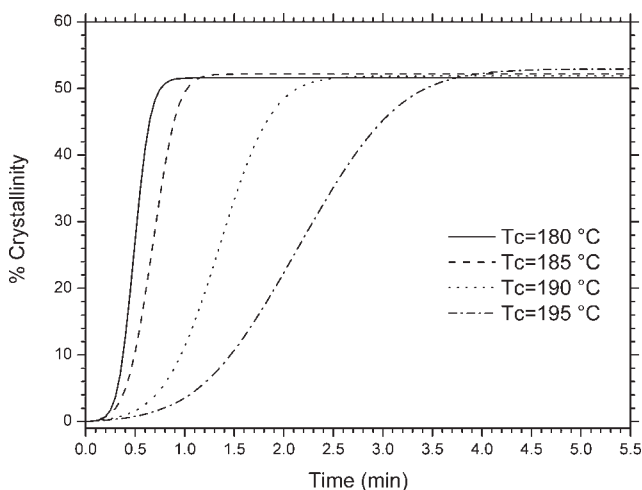


**Figure 2** Time evolution of the DSC crystallinity during isothermal crystallisation of PGA at various temperatures.

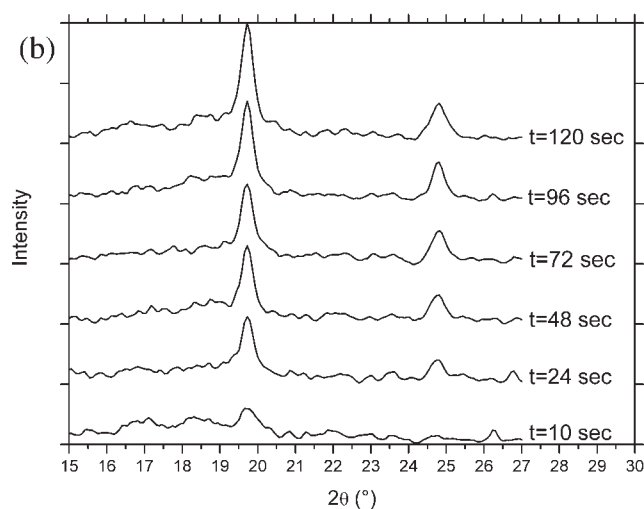
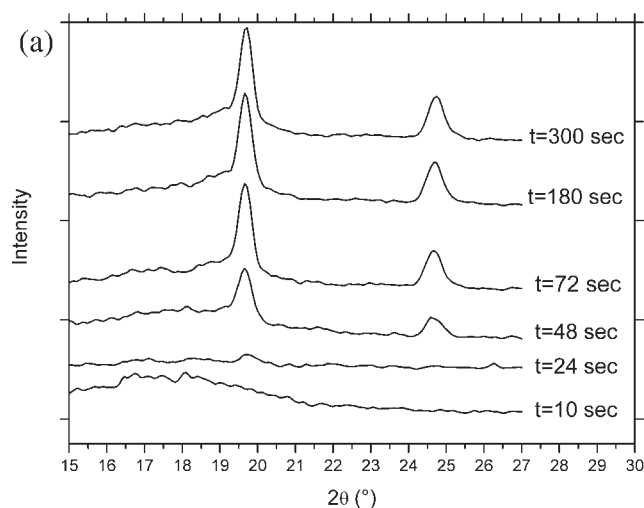


**Figure 3** (a) Time evolution of the WAXS intensity profiles during isothermal crystallization of PGA at 195°C; (b) time evolution of the WAXS intensity profiles during isothermal crystallization of PGA at 180°C.

sample crystallized at 195°C these peaks appear later, indicative of a faster crystallization rate at the lowest temperature (180°C), in agreement with our calorimetric results.

Figure 4 shows the time evolution of the X-ray crystallinity for PGA crystallized at 180°C and 195°C obtained with the following equation<sup>12</sup>

$$X_c = \frac{\int_a^b I_c(2\theta) d2\theta}{\int_a^b I(2\theta) d2\theta} \quad (2)$$

where  $I_c(2\theta)$  is the intensity scattered by the crystallites and  $I(2\theta)$  is the total diffracted intensity in the range  $2\theta = a$  to  $2\theta = b$ . To obtain  $I_c(2\theta)$  and  $I(2\theta)$  we followed the method described by Murthy and Minor<sup>13</sup> in which combinations of Gaussian and/or Lorentzian curves are fitted to the crystalline and amorphous parts of the diffraction pattern. The

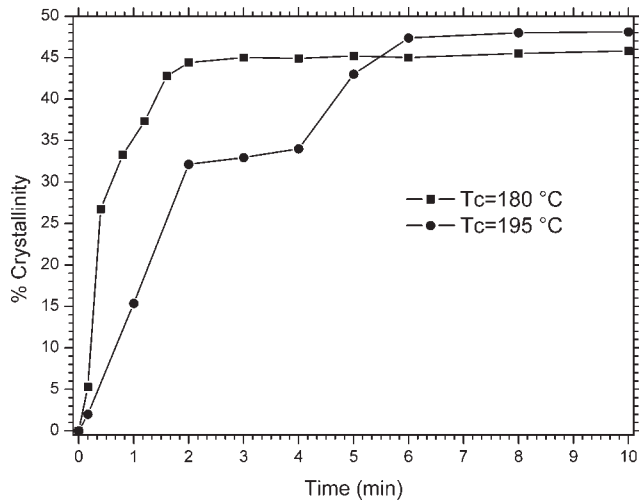


**Figure 4** Time evolution of the WAXS crystallinity during isothermal crystallization of PGA at 180°C and 195°C.

amorphous pattern was obtained from a sample in the molten state. The fitting parameters are obtained using a least squares fitting procedure described by Bevington<sup>14</sup> and the integrals in eq. (2) were evaluated numerically adapting the QDAGS IMSL Fortran subroutine for this particular task, with  $a = 17^\circ$  and  $b = 27^\circ$ . Figure 4 recalls the shape curves of the crystallinity obtained by DSC (Fig. 2) and both techniques indicate that the final crystallinity of the specimens is about 50% at the crystallization temperatures under consideration.

Figure 5 (a,b) show the time resolved SAXS intensity profiles for PGA crystallized at 180°C and 195°C, respectively. As can be seen, the intensities of the peaks at different stages during crystallization at 180°C are weak, whereas at 195°C strong peaks are well defined and can be associated with a lamellar structure.<sup>15</sup>

The SAXS data can be conveniently analyzed using the one-dimensional correlation function ( $\gamma_1$ ) obtained by assuming a model of single stack of lamella consisting of alternating parallel crystalline and amorphous regions. Ignoring the smearing effect due to the slit geometry the correlation function is obtained by Fourier transform of SAXS profile given by<sup>15</sup>

$$\gamma_1(x) = \frac{4\pi \int_0^\infty I(s)s^2 \cos(2\pi xs) ds}{Q} \quad (3)$$

where  $s = 2 \sin \theta / \lambda$  is the scattering vector,  $I(s)$  the observed intensity distribution, and  $Q$  the invariant given by

$$Q = 4\pi \int_0^\infty I(s)s^2 ds \quad (4)$$

Since the SAXS data are collected in a finite angular range, it is necessary to extrapolate to both low and high  $s$  values before Fourier transformation. The extrapolation to high  $s$  values was carried out with the aid of Porod's law given by<sup>15</sup>

$$\lim_{s \rightarrow \infty} [K - (I - I_b)s^4 \exp(\sigma^2 s^2)] = 0 \quad (5)$$

$$\int_0^\infty [K - (I - I_b)s^4 \exp(\sigma^2 s^2)] ds = 0 \quad (6)$$

where  $K$  is a constant,  $I_b$  is the contribution to the total scattering arising from inhomogeneous density fluctuations and  $\sigma$  is related to the thickness of the crystal/amorphous interface.<sup>16</sup> Once the parameters in eqs. (5) and (6) are obtained the invariant and the one-dimensional correlation function can be easily obtained with the aid of eqs. (3) and (4) and the long period ( $L$ ) can be estimated from the first

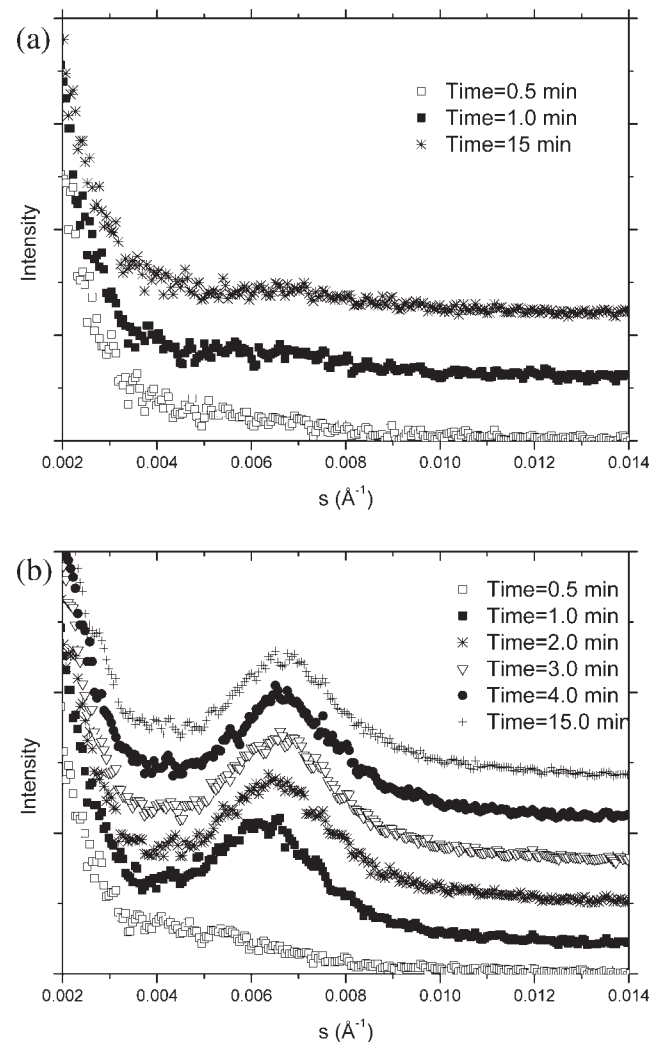


**Figure 5** (a) Time evolution of the SAXS intensity profiles during isothermal crystallization of PGA at 180°C; (b) time evolution of the SAXS intensity profiles during isothermal crystallization of PGA at 195°C.



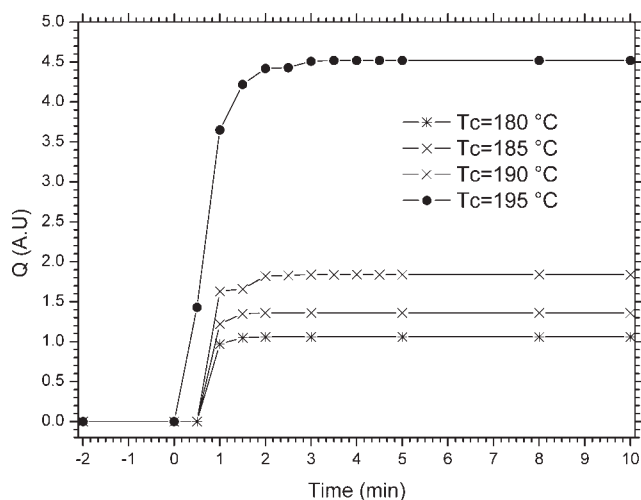


**Figure 6** Time evolution of the invariant ( $Q$ ) during isothermal crystallization of PGA at various temperatures.

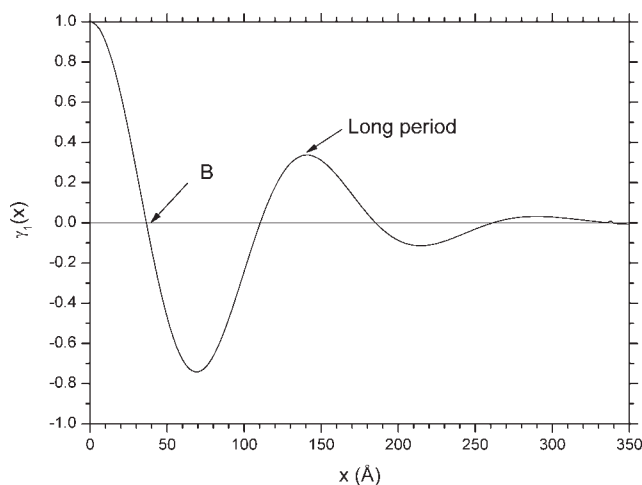
maximum of  $\gamma_1(x)^{15}$  as will be shown later in this section.

Figure 6 shows the time evolution of the invariant for PGA crystallized at various temperatures. As can be seen,  $Q$  decreases with decreasing the crystallization temperature due to the smaller total scattering power at low angles, indicative of a smaller difference in electron density between the amorphous and crystalline phases.<sup>12</sup> Hence, it would be expected that by increasing the degree of supercooling  $Q$  would drop to zero, quenching the “structure” of the molten state, hindering the formation of crystals and consequently of the lamellar structure. This was confirmed by extruding PGA fibers at 240°C, quenching them in a water bath at room temperature, obtaining amorphous PGA fibers with no evidence of a lamellar structure and crystallinity. As we will see in the following section, this is very important to make highly oriented PGA fibers.

Figure 7 shows an example of the analysis of the SAXS data following the method of the one dimensional correlation function [eq. (3)]. From the first maximum in the correlation function the long period ( $L$ ) can be obtained as mentioned earlier. Parameter  $B$  in eq. (7) below is obtained from the position of the first intercept of the correlation function with the  $x$ -axis in Figure 7.<sup>17</sup> Repeating the same analysis for various frames and crystallization temperatures, it is possible to obtain the time evolution of the long period and the thickness of the amorphous ( $L_a$ ) and crystalline ( $L_c$ ) regions with the aid of:<sup>17</sup>

$$\frac{B}{L} = x_{cl}(1 - x_{cl}) \quad (7)$$

where  $x_{cl}$  is defined by



**Figure 7** Example of the analysis of the SAXS data following the method of the correlation function. PGA crystallized at 195°C for 5 min.

$$L_a = (1 - x_{cl})L \quad \text{and} \quad L_c = x_{cl}L \quad (8)$$

Equation (7) is quadratic in  $x_{cl}$  and two solutions can be obtained. The sum of these two solutions is equal to 1 and only one of these corresponds to the lamellar thickness. Assuming that the appropriate solution is  $x_{cl} > 0.5$  is equivalent to assume that the lamellar stack model is adequate to describe the morphology developed during crystallization consisting of crystalline lamellae separated by interlamellar amorphous regions, with adjacent lamellar stack separated by amorphous material.<sup>17</sup>

Figure 8 shows the variations of  $L$ ,  $L_a$ , and  $L_c$  for PGA crystallized at 195°C. As can be seen initially the long period decreases rapidly and after about 2

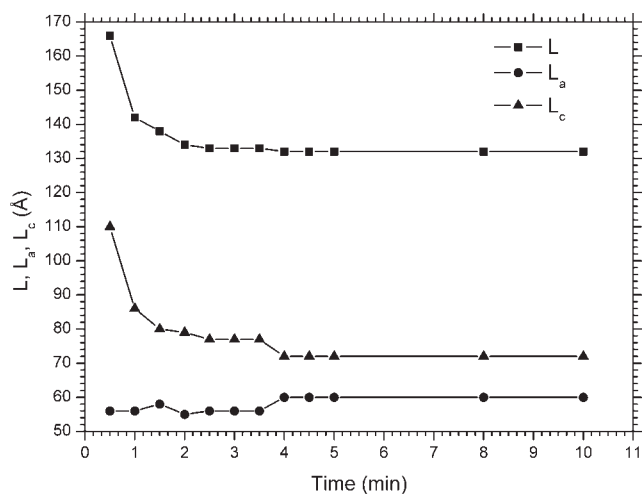


**Figure 8** Time evolution of the long period ( $L$ ) and the dimensions of the amorphous and crystalline regions ( $L_a$  and  $L_c$ , respectively) during isothermal crystallization of PGA at 195°C.

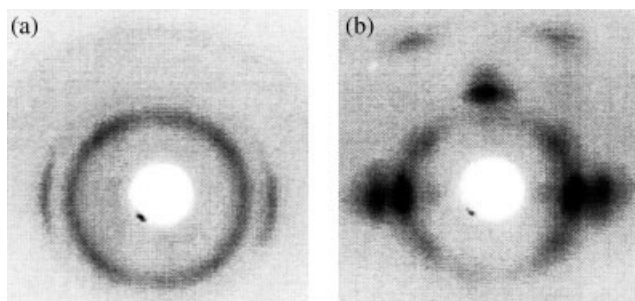


**Figure 9** (a) WAXS photographs of drawn PGA fibers obtained from an isotropic semicrystalline fiber subsequently drawn using the zone drawing technique; (b) WAXS photographs of drawn PGA fibers obtained from an isotropic amorphous fiber subsequently drawn using the zone drawing technique.

min it achieves a constant value of 132 Å. The lamellar thickness shows a similar behavior but in contrast the amorphous layer thickness shows significantly less variations during crystallization. A possible explanation is the insertion of thinner lamellae within the first 2 min of crystallization, which coincides with the rapid development of the invariant as can be seen in Figure 6, reducing the values of  $L$  and  $L_c$ . Similar observations have been carried out by Wang et al. during isothermal crystallization of PGA at 200°C.<sup>10</sup> From this analysis it was found that  $L_c$  at the end of the crystallization is approximately 70 Å, independent of crystallization temperature in the temperature range 180–195°C.

### Structure and mechanical properties of PGA fibers

Figure 9(a,b) show the WAXS photographs of drawn PGA fibers. Figure 9(a) was obtained from fibers initially 50% crystalline (obtained by annealing amorphous fibers at 110°C for 30 min) and subsequently drawing them at 110°C using the zone drawing technique, obtaining fibers with modulus of 7 GPa. Figure 9(b) on the other hand was obtained from fibers initially amorphous and subsequently drawn under the same conditions, obtaining fibers with modulus in the range of 20–25 GPa.<sup>18,19</sup> It is evident that drawing fibers with a high degree of crystallinity results in poor molecular orientation. Molecular orientation and enhancement of the mechanical properties of PGA are most effective by drawing amorphous PGA above the glass transition temperature.

### CONCLUSIONS

The crystallization rate of PGA decreases with crystallization temperature in the temperature range 180–195°C. The crystallinity measured by DSC agrees well with that measured by WAXS, approaching a limiting value of about 50% independent of the crystallization temperature in the range from 180 to 195°C. SAXS analysis indicates that PGA develops a lamellar structure during crystallization with a final crystal thickness approaching a limiting value of 70 Å, independent of the crystallization temperature in the range from 180 to 195°C. We showed that by increasing the degree of supercooling it is possible to hinder the formation of the lamellar structure and crystals, resulting in a less ordered structure. We found that molecular orientation and enhancement of the mechanical properties in PGA during plastic deformation is most effectively achieved by drawing amorphous PGA at 110°C.

We would also like to thank Mr. Anthony Gleeson for station support at the CLRC Daresbury Laboratories.

### References

1. Vert, M.; Li, S. M.; Spenlehauer, G.; Guerin, P. *J Mater Sci: Mater Med* 1992, 3, 432.
2. Athanasiou, K. A.; Agrawal, C. M.; Barber, F. A.; Burkhart, S. S. *Arthroscopy* 1998, 14, 726.
3. Middleton, J. C.; Tipton, A. J. *Biomaterials* 2000, 21, 2335.
4. Chatani, Y.; Suehiro, K.; Okita, Y.; Tadokoro, H.; Chujo, K. *Die Makromol Chem* 1968, 113, 215.
5. Montes de Oca, H.; Ward, I. M.; Klein, P. G.; Ries, M. E.; Rose, J.; Farrar, D. *Polymer* 2004, 45, 7261.
6. Grabar, D. G. *Microscope* 1970, 18, 203.
7. Chu, C. C. *Polymer* 1980, 21, 1480.
8. Cohn, D.; Younes, H.; Marom, G. *Polymer* 1987, 28, 2018.
9. Gilding, D. K.; Reed, A. M. *Polymer* 1979, 20, 1459.
10. Wang, Z. G.; Hsiao, B. S.; Zong, X.; Yeh, F.; Zhou, J.; Dormier, E.; Jamiolkowsky, D. D. *Polymer* 2000, 41, 621.
11. Montes de Oca, H.; Ward, I. M. *Polymer* 2006, 47, 7070.
12. Alexander, L. E. *X-ray Diffraction Methods in Polymer Science*; Wiley: New York, 1969.
13. Murthy, N. S.; Minor, H. *Polymer* 1990, 31, 996.
14. Bevington, P. R. *Data Reduction and Error Analysis for the Physical Sciences*; McGraw-Hill: New York, 1969.
15. Vonk, C. G. *Synthetic Polymers in Small Angle X-ray Scattering*; Glatter, O.; Kratky, O., Eds.; Academic Press: London, 1982.
16. Krüger, K. N.; Zachmann, G. G. *Macromolecules* 1993, 26, 5202.
17. Verma, R.; Marand, H.; Hsiao, B. S. *Macromolecules* 1996, 29, 7767.
18. Rose, J. WO 2003/064531.
19. Rose, J. WO 2005/014718.